JOURNAL OF THERMOPHYSICS AND HEAT TRANSFER
Vol. 20, No. 1, January–March 2006

Parameters Affecting Turbulent Film Cooling—Reynolds-Averaged Navier–Stokes Computational Simulation

Shadi Mahjoob*
Aerospace Research Institute, Ministry of Sciences, Research, and Technology, 14665-834 Tehran, Iran
and
Mohammad Taeibi-Rahni†
Sharif University of Technology, 11365-8639 Tehran, Iran

Film cooling of surfaces appears in many applications. For instance, it is one of the most effective methods to improve the efficiency of gas turbines. As a fundamental study, two different types of film cooling (slot and discrete holes injections) are numerically simulated here. A flat surface is used to model a small portion of a gas turbine blade. Incompressible, stationary, viscous, turbulent flow is assumed using the STAR-CD software with the standard k–ε model and a cell-centered finite volume method on a nonuniform structured grid. The jet flow Reynolds number, based on the jet's hydraulic diameter, is 4.7×10^3. The study of the injection angle and the velocity ratio shows that the optimum film cooling occurs at jet angle of about 30 deg. However, the optimal velocity ratios of about 1.5 for slot injection and about 0.5 for discrete holes injection have been obtained. On the other hand, the study of jet-exit aspect ratio in discrete holes injection shows that stretching the hole in spanwise direction increases the film-cooling effectiveness. Also, the study of jet spacing in spanwise direction shows that decreasing the jet spacing increases the film-cooling effectiveness, but not as much as the jet aspect ratio.

Nomenclature

$C_{1\varepsilon}$	=	constant
$C_{2\varepsilon}$	=	constant
D	=	side of the jet exit (0.0127 m)
G_k	=	generation of turbulent kinetic energy caused by the mean velocity gradients
K	=	thermal conductivity
k	=	turbulent kinetic energy
L	=	length scale
R	=	velocity ratio ($V_{\text{Jet}}/V_{\text{CF}}$)
r	=	blowing ratio ($\rho_{\text{Jet}}V_{\text{Jet}}/\rho_{\text{CF}}V_{\text{CF}}$)
U	=	velocity in X direction
u_i, u_j	=	velocity in i and j directions
ε	=	rate of dissipation
η	=	film-cooling effectiveness $[(T_{\text{AW}} - T_{\text{CF}})/(T_{\text{Jet}} - T_{\text{CF}})]$
θ	=	cooling efficiency $[(T - T_{\text{CF}})/(T_{\text{Jet}} - T_{\text{CF}})]$
μ	=	absolute viscosity coefficient
μ_T	=	eddy viscosity coefficient
ρ	=	density
σ_k	=	turbulent Prandtl number for k
σ_ε	=	turbulent Prandtl number for ε
τ_{ij}	=	Reynolds-stress tensor
$()_{\text{AW}}$	=	designates adiabatic wall
$()_{\text{CF}}$	=	designates crossflow
$()_{\text{Jet}}$	=	designates jet

I. Introduction

FILM cooling is used in various applications including combustion chambers' walls, the blades of gas turbines, etc. On the other hand, one of the most useful methods to improve jet engine efficiency is to increase the turbine entrance temperature. However, the inlet temperature is limited by the potential structural failure of the engine components, especially, the first stage of the turbine blades. The cooling air reduces the capacity of the turbine to drive the compressor because of the lower temperature at which it enters the turbine. Furthermore, the cooling air mixes with the mainstream turbine air and causes aerodynamic losses. Both of these effects are so strong that vigorous steps are taken to minimize them.[1]

In general, a hot surface can be cooled either internally or externally. The external cooling is usually performed by creating a film of cool air near the surface, which is called film cooling. Because internal cooling of the blades is not always efficient, film cooling is used in more modern applications. In film cooling, cool air is injected into the crossflow very near the surface through some rows of slot or discrete holes. Because, in slot injection film cooling, the cooling jet is injected all along the span, it results in a better performance. However, because of structural considerations, rows of discrete film cooling holes are usually used. However, film cooling with discrete holes has problems like nonuniformity of cooling in spanwise direction and excessive penetration of the cooling jets into the mainstream. To overcome these difficulties, rows of rectangular or expanded-shape holes are mostly used in more recent years.[2]

Gartshore et al.[3] studied the effects of two different hole shapes (circular and squared). Their results show that the squared holes are slightly superior (from cooling point of view) only very close to the injection point and only at low velocity ratios, for example, $R = 0.5$. Note, many people have compared expanded-shape and circular cross-sectional film-cooling holes, whereas only a few have compared squared and rectangular film-cooling holes.

Muldoon and Acharya[4] and Licu et al.[5] investigated flow characteristics and film-cooling performance downstream of rectangular holes, using numerical and experimental methods, respectively. Cho et al.[2] studied film cooling using jet injection of 90 deg with squared and rectangular holes. They investigated local heat-transfer characteristics inside the holes with variations of the blowing ratio and the jet Reynolds number.

Although film cooling offers an excellent compromise between the protection of the walls and the aerodynamic efficiency, it can even be ineffective if the related parameters are not chosen properly. Some of the most important factors that have gained much of the

Received 18 November 2004; revision received 17 March 2005; accepted for publication 24 March 2005.

*Senior Research Engineer, Havafaza Alley, Mahestan Street, Iranzamin Street, Shahrak Ghods and Faculty Member Aerospace Research Institute, Ministry of Sciences, Research, and Technology, 14665-834 Tehran, Iran; shmahjoob@ari.ac.ir.

†Associate Professor, Aerospace Engineering Department, Azadi Avenue and Faculty Member Aerospace Research Institute; taeibi@sharif.edu.

researchers' attention are cooling jet injection angle,[6] compound injection angle,[7,8] blowing ratio,[9,10] spanwise and streamwise hole spacing,[11,12] length of the cooling jet channel,[13–18] boundary-layer thickness,[19] wall curvature,[19] and turbulence.[15,20–22]

In the present work, two different methods of film cooling, namely, slot injection and discrete holes injection, were numerically simulated. Because both methods are investigated at nearly the same conditions, their related results can be easily compared. In each method, velocity ratios of 0.5, 1, and 1.5 and jet injection angles of 30 and 90 deg were studied, and the optimum velocity ratio and the optimum jet injection angle were obtained. Then, to study the effects of the aspect ratio of the jet-exit cross section and the spanwise spacing of the jets, five different rectangular and squared sections were compared at the optimum velocity ratio and optimum injection angle. Note, most of the work of researchers on jet cross-section shape has been done at the jet angle of 90 deg, which is not the optimum case.

II. Computational Geometric Modeling

Two different geometries were used in this study. The basic geometry, which is similar to the one used by Ajersch et al.,[23] is shown in Fig. 1a. The effects of jet injection angle and velocity ratio were studied using this geometry in both cases of slot injection and hole injection film cooling. The computational domain used was a $45D \times 25D \times 3D$ cube with a $1D \times 1D$ jet channel. In slot injection film cooling, the jet channel is stretched all along the spanwise direction. In both jet injection angles of 30 and 90 deg, the depth of the jet channel was taken to be $5D$.

The second geometry used is for studying the jet cross-section aspect ratio. In this geometry, which is $45D \times 25D \times 4.5D$, five different cases of jet-exit cross sections were used (Fig. 1b). These dimensions were chosen such that the jet Reynolds number stayed the same as in the first geometry (4.7×10^3). Note, in both geometries we were using a spanwise jet spacing of three times the biggest width of jet cross section ($3 \times D$ in basic geometry and $3 \times 3/2D$

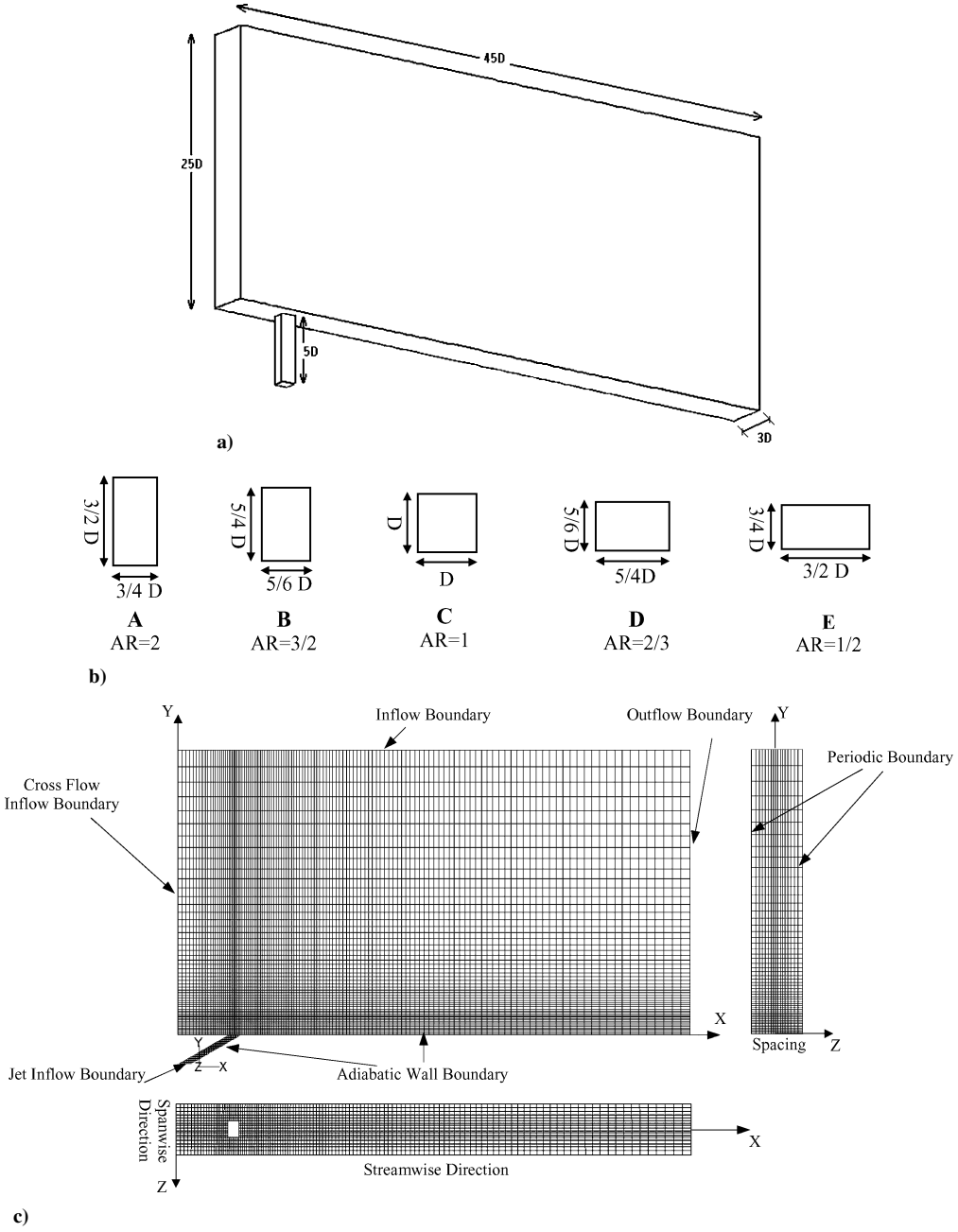

Fig. 1 Geometric modeling and the boundary conditions used: a) basic geometry, b) different jet aspect ratios (AR: ratio of spanwise to streamwise lengths), and c) grid.

in second geometry). In addition, to study the jet spacing effects the results of the squared hole injection with jet spacing of $3D$ is compared with that of $4.5D$. Note, in all cases studied the distance between the main inflow boundary to the beginning of the jet is set to $4.5D$.

III. Flow Characteristics

The turbulent flow considered here was incompressible and stationary with the following conditions. The cooling jet velocity was taken to be 5.5 m/s, and the jet flow Reynolds number, based on the jet's hydraulic diameter, was 4.7×10^3. The crossflow velocity was calculated based on the velocity ratio R. The thickness of the boundary layer was estimated from the experimental results of Ajersch et al.[23] and was about $2D$. The temperature of the cross and the jet flows were 1000 and 300 K, respectively. The density and the viscosity coefficient were 1.204 kg/m^3 and 1.7894×10^{-5}, respectively.

IV. Governing Equations

In this study, the following forms of the governing equations including continuity, momentum, and energy, were used:

$$\frac{\partial}{\partial x_i}(u_i) = 0 \tag{1}$$

$$\rho \frac{\partial}{\partial x_j}(u_i u_j) = -\frac{\partial p}{\partial x_i} + \frac{\partial \tau_{ij}}{\partial x_j} + \rho g_i + F_i \tag{2}$$

$$\rho \frac{\partial}{\partial x_i}(u_i h) = \frac{\partial}{\partial x_i}\left[K \frac{\partial T}{\partial x_i}\right] + u_i \frac{\partial p}{\partial x_i} + \tau_{ij} \frac{\partial u_i}{\partial x_j} \tag{3}$$

where

$$\tau_{ij} = \left[\mu_{\text{eff}}\left(\frac{\partial u_i}{\partial x_j} + \frac{\partial u_j}{\partial x_i}\right)\right] \tag{4}$$

$$\mu_{\text{eff}} = \mu + \mu_T \tag{5}$$

The standard k–ε model was used in this study. The turbulent kinetic energy k and its rate of dissipation ε are obtained from the following transport equations, proposed by Launder and Spalding[24]:

$$\rho \frac{\mathrm{D}k}{\mathrm{D}t} = \frac{\partial}{\partial x_i}\left[\left(\mu + \frac{\mu_t}{\sigma_k}\right)\frac{\partial k}{\partial x_i}\right] + G_k - \rho\varepsilon \tag{6}$$

and

$$\rho \frac{\mathrm{D}\varepsilon}{\mathrm{D}t} = \frac{\partial}{\partial x_i}\left[\left(\mu + \frac{\mu_t}{\sigma_\varepsilon}\right)\frac{\partial \varepsilon}{\partial x_i}\right] + C_{1\varepsilon}\frac{\varepsilon}{k}(G_k) - C_{2\varepsilon}\rho\frac{\varepsilon^2}{k} \tag{7}$$

In addition, the standard wall functions, based on the work of Launder and Spalding[25] were used.

V. Boundary Conditions

In all cases studied, four different boundary conditions were used (Fig. 1c), namely, inflow, outflow, periodic, and no slip. Also, adiabatic wall condition was used in the energy equation. At the crossflow inflow boundary, up to $2D$ from the wall, the 1/7 power law was used, while uniform flow was considered for the rest of the flow there. The square root of turbulent kinetic energy at the inflow boundaries was based on Ajersch et al.[23] experimental data. For $R = 1$ or 1.5, they assumed it to be $0.02V_{\text{CF}}$, whereas for $R = 0.5$ they used $0.012V_{\text{CF}}$, while ε was calculated from the following relation:

$$\varepsilon = C_\mu^{\frac{1}{4}}(k^{\frac{3}{2}}/l) \tag{8}$$

$$l = 0.07L \tag{9}$$

$$C_\mu = 0.09 \tag{10}$$

Table 1 Number of grid cells for five different grids studied

Number of cells	Main domain			Jet channel		
	N_X	N_Y	N_Z	N_X	N_Y	N_Z
17,000	63	27	10	4	14	4
30,000	84	35	10	4	19	4
68,000	100	45	15	5	25	5
120,000	126	55	17	7	30	7
200,000	150	63	21	9	35	9

VI. Computational Methodology

In this work, an implicit cell-centered finite volume method was used. Also, the SIMPLE algorithm (with underrelaxation coefficients) was implemented in the overall discretization of the equations. Note, all of the schemes used were second order. However, in order to reduce the dispersion errors (and also to increase the speed of the computations), the multigrid approach has also been used.[26] Also, in all cases studied, a nonuniform structured grid was used (Fig. 1c).

VII. Code Validation and Grid-Resolution Study

To validate the code, velocity and kinetic turbulent energy results obtained from our simulation were compared with those of the available experimental and computational data of Ajersh et al.[23] for velocity ratio of 0.5 at the jet injection angle of 90 deg. The comparison of the computational-fluid-dynamics results with the experimental data shows relatively high accuracy of our simulations (Figs. 2 and 3). Note, the quality and the accuracy of our results are better than those of the computational results of Ajersch et al.[23] Of course, turbulent kinetic energy (Fig. 3) is a very sensitive parameter, and thus its prediction is not always easy, especially for flows such as the ones simulated here, with excessive rate of strain (e.g., flows with high streamline curvature, highly vortical flows), and with multiple length scales. Of course, jet-crossflow interactions are complicated at high jet injection angles, for example, 90 deg. Thus, this shortcoming is not noticeable at low injection angles, for example, 30 deg.

Note, because the Reynolds number of the main flow is high and the adiabatic wall assumption is used, the effects of the convection heat transfer are much stronger than those of the diffusion heat transfer. Therefore, validation of the flow hydrodynamics can pretty much ensure that the film-cooling effectiveness results are also accurate enough.

The grid independency of the squared jet cross section for the basic geometry (with the jet spacing of $3D$) was studied using five different grids (Table 1). Because the flow complexity and the jet into crossflow interactions occur mostly near the wall (especially over and behind the jet), the grid was clustered there in Y direction, as well as at the jet exit in X and Z directions. In Fig. 4, the results related to different grids used are compared. This figure indicates that, by increasing the cell numbers from 120,000 to 200,000, the adiabatic film-cooling effectiveness η, which is the major parameter studied in this work, almost remains constant. However, further decrease of the number of cells changes the film-cooling effectiveness considerably. Therefore, a 120,000-cells grid was used, whose distribution (especially in the sensitive regions, e.g., near the wall and the jet channel) is the same as that of the previous works (Refs. 21 and 23). A similar study (not shown here) indicated that for the second geometry (with the jet spacing of $4.5D$) 210,000-cells grid was more suitable.

VIII. Results

In this work, the physics of the flow and the film-cooling effectiveness of two kinds of flat-plate film cooling (slot and discrete holes injections) for different velocity ratios and jet injection angles have been studied. The film-cooling results of these two cases have also been compared. For the discrete holes, the effects of the jet aspect ratio and the jet spacing have also been investigated.

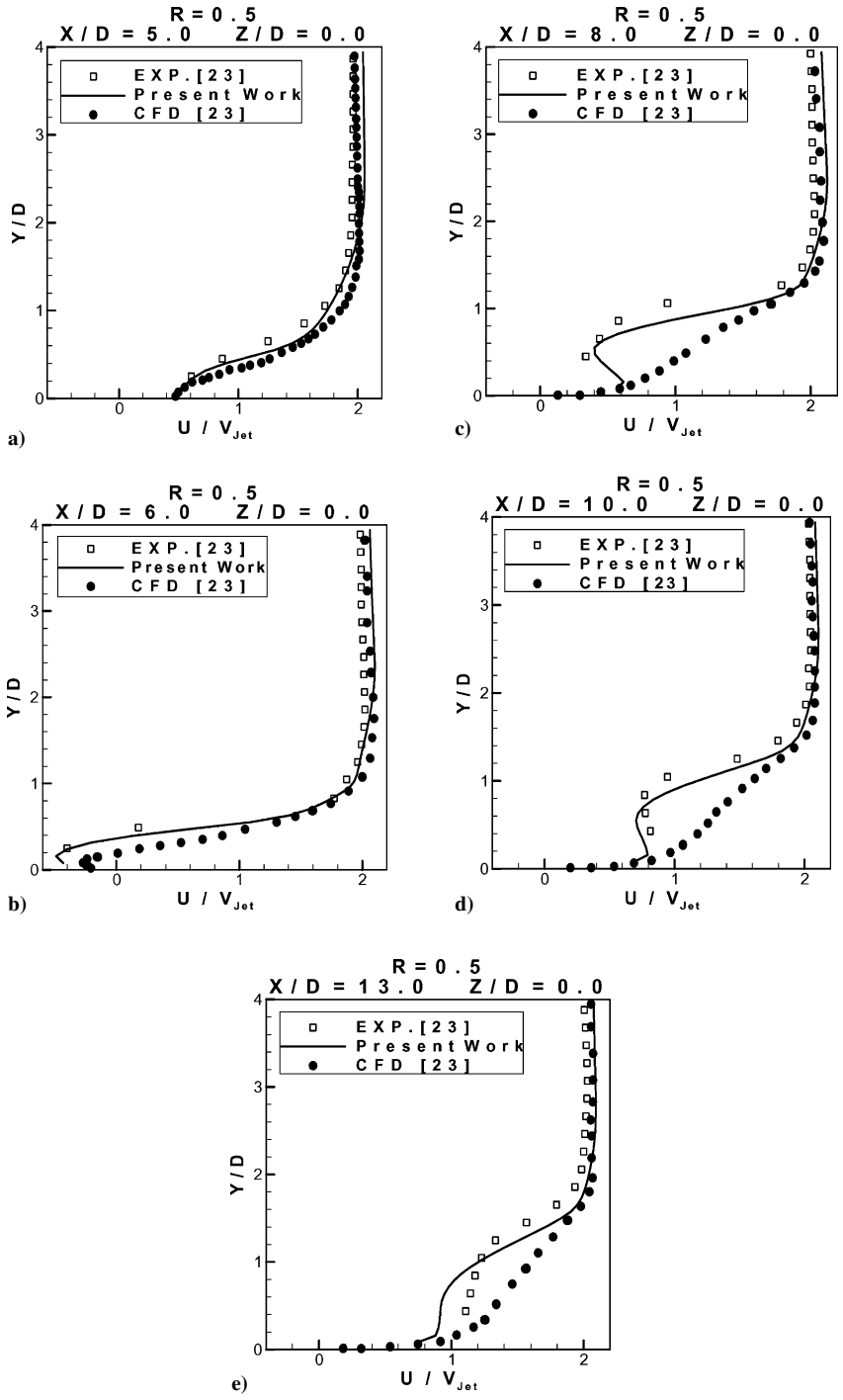

Fig. 2 Comparison of streamwise velocity (U/V_{Jet}) for $Z/D = 0$, with velocity ratio of 0.5 and jet injection angle of 90 deg: a) $X/D = 5.0$, b) $X/D = 6.0$, c) $X/D = 8.0$, d) $X/D = 10.0$, and e) $X/D = 13.0$.

A. Slot Injection Film Cooling

As part of our study, flat-plate slot injection film cooling has been simulated in six different situations, namely, jet injection angles of 30 and 90 deg with velocity ratios of 0.5, 1, and 1.5. The results indicate that, for all of these velocity ratios, for jet injection angle of 30 deg the penetration of the jet into the main flow is minimal because in this case the cooled flow stays adjacent to the wall. However, by changing the jet injection angle to 90 deg, the cooling jet influences the main flow, considerably. Therefore, the height of the jet increases, and the region over and far from the wall becomes cool, rather than the wall itself. Also, flow separation occurs downstream of the jet (Fig. 5).

In general, increasing the velocity ratio enhances the jet penetration, and thus the centerpoint of the reverse flow region (the most cooled region) will be situated farther away from the wall, as the velocity ratio increases.

Figure 6 shows the film-cooling effectiveness for different injection angles and different velocity ratios. Note, at velocity ratios of 1 and 1.5 the increase in the jet injection angle decreases the effectiveness of film cooling. This is because the reverse flow is generated behind the jet such that the cool air penetrates into the region far from the wall, rather than staying adjacent to the wall. At velocity ratio of 0.5 however, the film-cooling effectiveness η for both the jet injection angles of 30 and 90 deg is very close, while being small. Also, in both jet injection angles the increase in the velocity ratio enhances the film-cooling effectiveness, especially at low angle of 30 deg. Therefore, the optimum film cooling, using slot injection, occurs at the jet injection angle of 30 deg and

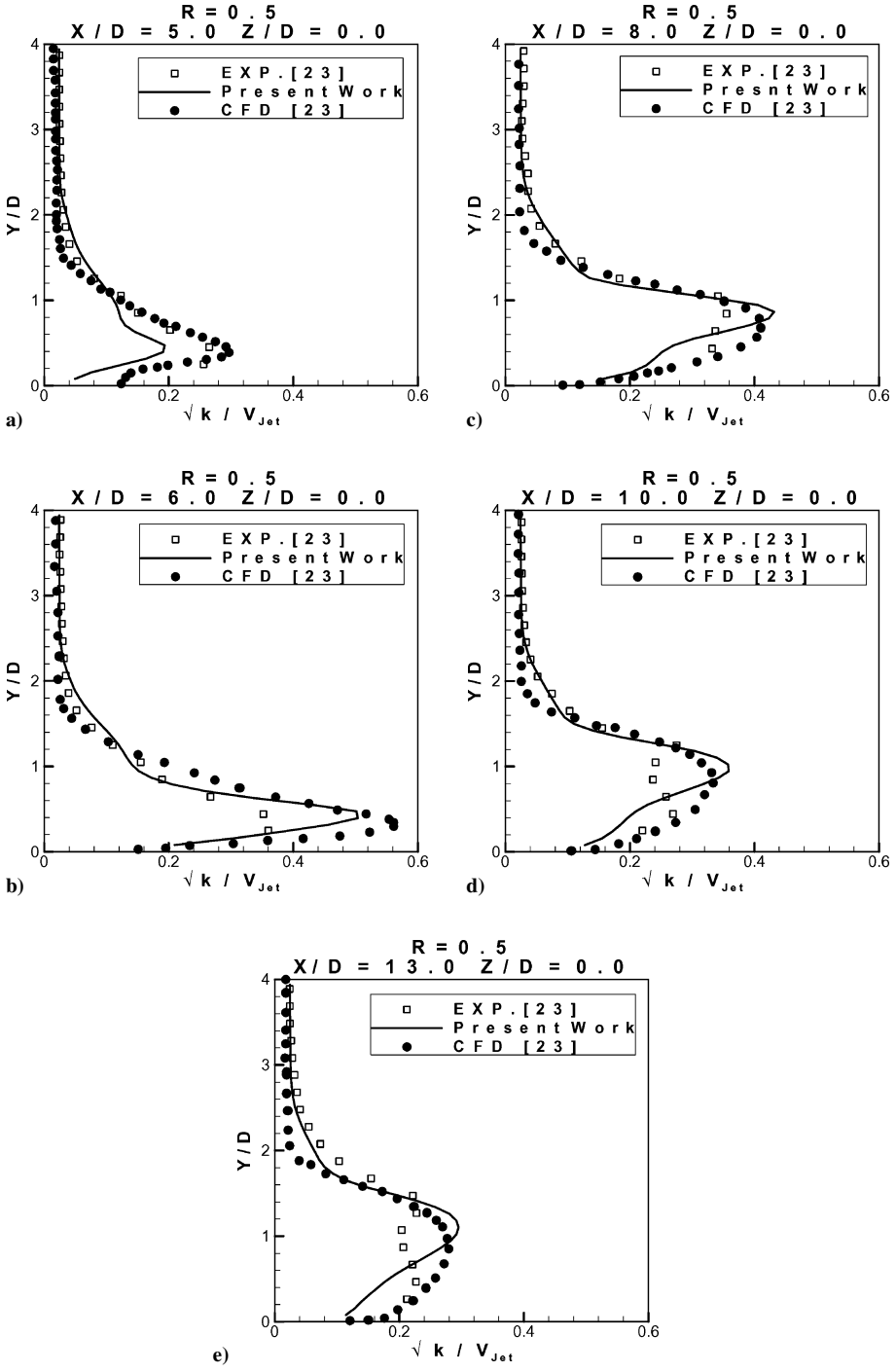

Fig. 3 Comparison of the square root of turbulence kinetic energy ($\sqrt{k}/V_{\text{Jet}}$) for $Z/D = 0$, with velocity ratio of 0.5 and jet injection angle of 90 deg: a) $X/D = 5.0$, b) $X/D = 6.0$, c) $X/D = 8.0$, d) $X/D = 10.0$, and e) $X/D = 13.0$.

at the velocity ratio of 1.5, while the worst case is the velocity ratio of 0.5.

B. Discrete Holes Injection Film Cooling

Similar to the slot injection technique, for injection angle of about 30 deg (for all three velocity ratios studied) the flow moves close to the wall. As expected, by increasing the jet angle to 90 deg the height of the jet increases considerably. However, because of the existence of a third dimension in discrete holes injection the physics of the flow is quite different from that of the slot injection jet (Fig. 7). Now, the cold fluid behind the jet traps in one of the two symmetrical spirals, which are moving along the wall downstream (instead of being trapped in the reverse flow region mentioned in the slot film cooling). However, there is a small reverse flow just behind the jet and below the spiral flow, which creates a wake region at the wall (Fig. 8).

While avoiding the cooling of the fluid far from the wall, we studied the dimensionless temperature variations in the region over and far from the wall, namely, the cooling efficiency θ for the first time to the authors' knowledge. Figure 9 shows the cooling efficiency at $Z = 0$ and $X = 6.5D$ ($1D$ after the jet) along the axes normal to the wall (Y). Note from this figure that for both 30- and 90-deg injection angles, by increasing the velocity ratio, the height of cooled flow increases, and thus the region above the wall is more influenced by the cooling flow. In other words, at the jet injection angle of 90 deg, the reverse flow becomes larger and occurs farther away from the wall.

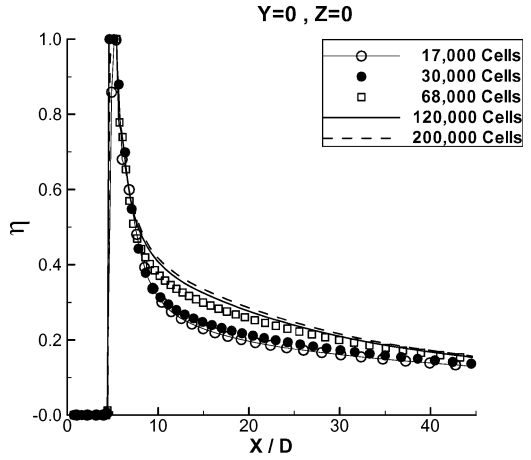

Fig. 4 Grid-resolution study: film-cooling effectiveness at the centerline ($Y = 0, Z = 0$).

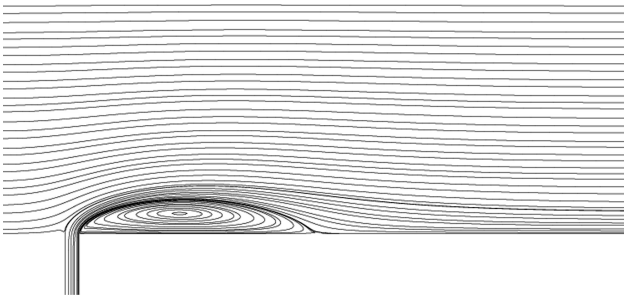

Fig. 5 Reverse flow generated in the slot film cooling for jet injection angle of 90 deg and velocity ratio of 1.5.

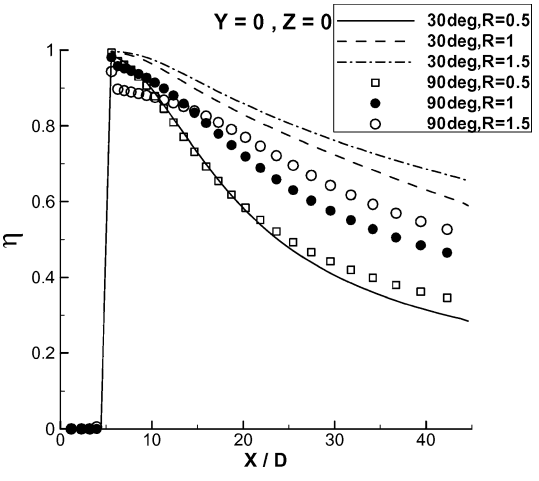

Fig. 6 Film-cooling effectiveness at the jet centerline ($Y = 0$ and $Z = 0$) at different jet angles and velocity ratios, using slot injection.

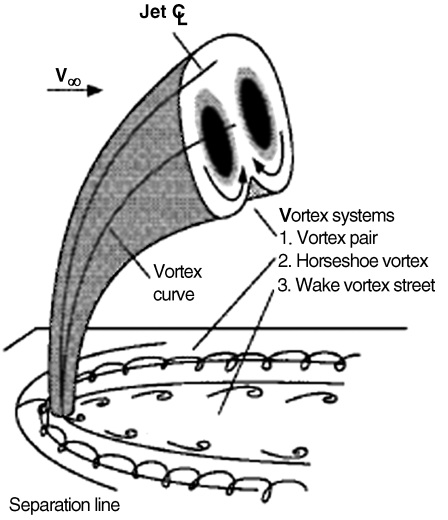

Fig. 7 Different vortices generated for the jet injection angle of 90 deg (Ref. 27).

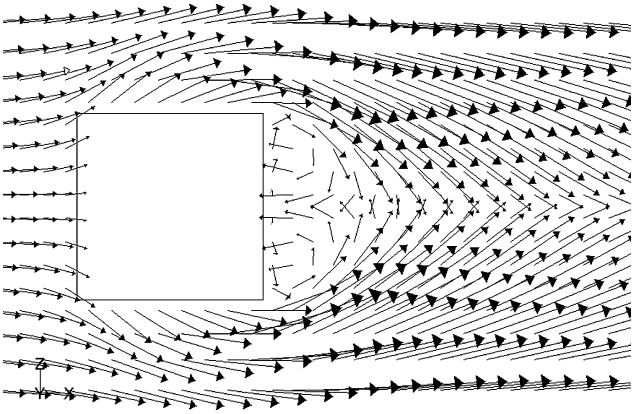

Fig. 8 Wall wake for the jet injection of 90 deg and the velocity ratio of 0.5, using discrete holes injection.

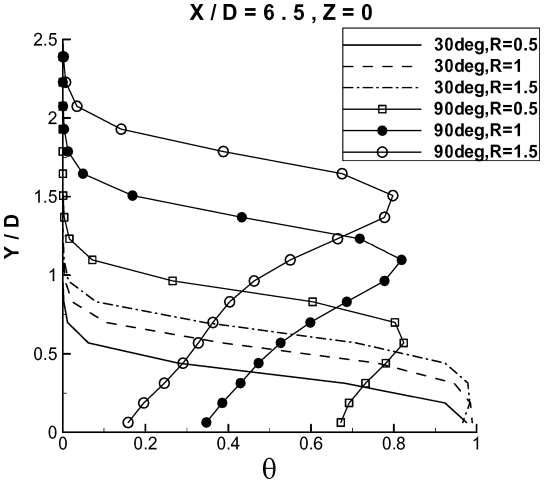

Fig. 9 Cooling efficiency at $X = 6.5D$ and $Z = 0$ for different jet angles and velocity ratios, using discrete holes injection.

This leads to a decrease in the effects of the reverse flow at the wall and thus smaller wake region at the wall. Figure 9 also shows that, at the jet injection angle of 90 deg, the maximum cooling efficiency θ is about 0.8 occurring relatively far from the wall, whereas, at the injection angle of 30 deg, it is about one occurring much closer to the wall. In other words, at 30-deg jet injection angle the cold fluid has cooled the wall more efficiently without influencing the flow far from the wall considerably.

On the other hand, Fig. 10 shows the film-cooling effectiveness η at the jet centerline along the streamwise direction. Note from this figure that, starting with the velocity ratio of 0.5 and injection angle of 30 deg, as the injection angle or the velocity ratio increases the film-cooling effectiveness in the region just downstream of the hole decreases. Therefore, the optimum film cooling occurs at the jet injection angle of 30 deg and at the velocity ratio of 0.5, whereas the worst case is the jet injection angle of 90 deg with the high velocity ratio of 1.5. Note, using a jet injection angle less than 30 deg or velocity ratio less than 0.5 decreases the efficiency.[21] Another point in this figure is that, at velocity ratios of 0.5 and 1, the jet angle of 30 deg has a longer (in streamwise direction) and thus more effective

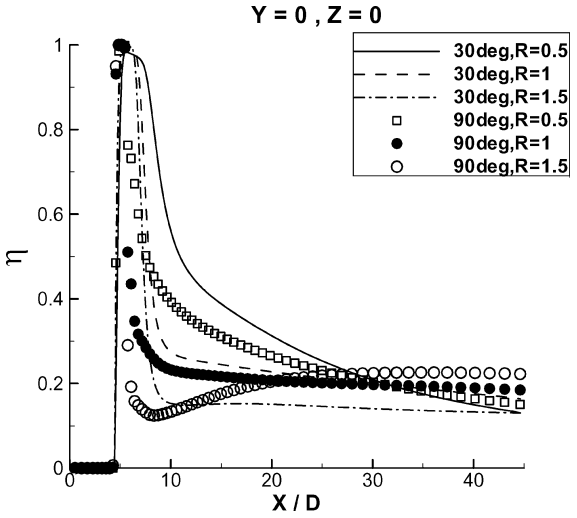

Fig. 10 Film-cooling effectiveness at the jet centerline ($Y = 0$ and $Z = 0$), for different jet injection angles and velocity ratios, using discrete holes injection.

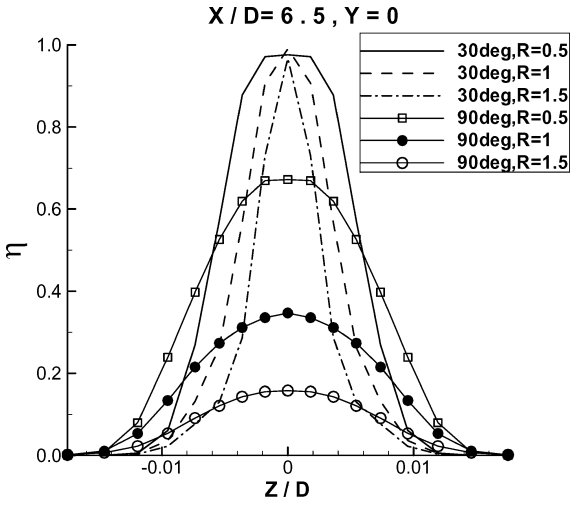

Fig. 11 Film-cooling effectiveness at $X = 6.5D$ and $Y = 0$, for different jet injection angles and velocity ratios, using discrete holes injection.

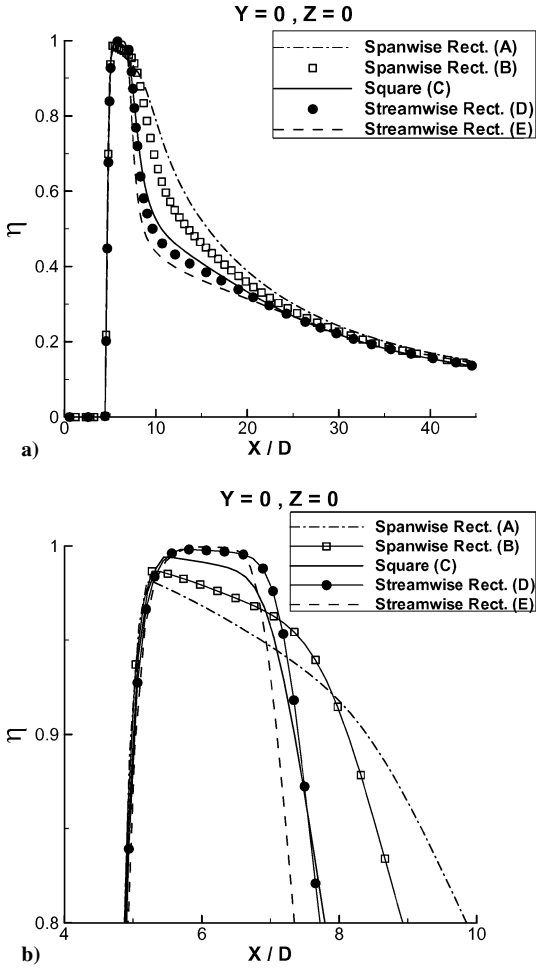

Fig. 12 Film-cooling effectiveness at the jet centerline ($Y = 0$ and $Z = 0$) for the jet angle of 30 deg and the velocity ratio of 0.5, using discrete holes injections with different aspect ratios: a) the whole graph and b) a part of graph a enlarged.

film cooling than those of 90 deg. However, it can be seen that at all velocity ratios, at far downstream ($x > 27D$), the jet angle of 90 deg has better film-cooling effectiveness. However, it is important that, in this region, the cooling effectiveness is less than 0.2 and it is thus inappropriate.

In spite of the disadvantages of using 90-deg injection angle, it has some advantages. Beside the fact that it is simpler for manufacturing purposes, it generates a wider distribution of film cooling in spanwise direction (Fig. 11), but because its value is small this advantage is not so important. Note also from Fig. 11 that, at the jet injection angle of 30 deg, as the velocity ratio is increased the distribution of the film cooling in spanwise direction decreases.

To investigate the effects of the jet cross-section's aspect ratio, the results of a squared cross section and four different rectangular cross sections have been compared at the optimum velocity ratio of 0.5 and the jet injection angle of 30 deg. Figure 12a shows that changing the jet cross section from spanwise rectangle (cases A and B) to square (case C) and also from square to streamwise rectangle (cases E and D) decreases the effective film-cooling length along the wall. Another point is that, in spanwise rectangular jets (cases A and B), film-cooling effectiveness is reduced from unity, just as the cold fluid crosses the jet (Fig. 12b), while, the streamwise rectangular jets (cases D and E) can sustain film-cooling effectiveness of unity at longer distances. However, after that, the film-cooling effectiveness of the streamwise rectangular jets (cases D and E) decreases quickly, whereas the rate of decrease in spanwise rectangular jets (cases A and B) is much lower.

Furthermore, by changing the jet cross section from spanwise rectangle (case A) to streamwise rectangle (case E) the height of cooled flow behind the jet is increased, and thus the fluid far from the wall also cools down (Fig. 13). In other words, the film cooling affects mostly the main flow rather than the fluid adjacent to the wall.

Figure 14 compares the film-cooling effectiveness of different jets in spanwise direction, at $X = 7D$ and $Y = 0$. As expected, because of their geometries the spanwise rectangular jets (cases A and B) have wider distributions of film cooling in comparison with other jets.

Another important point noticed in Figs. 12–14 is that, although the length and the width of both spanwise and streamwise rectangular jets (e.g. cases A and E) are the same, the difference between the results of the spanwise rectangular jet (case A) and the squared one (case C) is more than the difference between the results of the streamwise rectangular jet (case E) and the squared one (case C). In fact, the more the rectangular section stretches in the spanwise direction, the more rapidly the efficiency increases.

C. Spanwise Jet Spacing Effects

Another important parameter affecting film cooling is the distance between adjacent jets in spanwise direction. To study this effect, the results of two different film-cooling cases, one having a jet spacing of $3D$ (say case G) and the other having a jet spacing of $4.5D$ (case C) with a jet injection angle of 30 deg and a velocity ratio of 0.5, have been compared (Figs. 15 and 16). Note from Fig. 15 that increasing

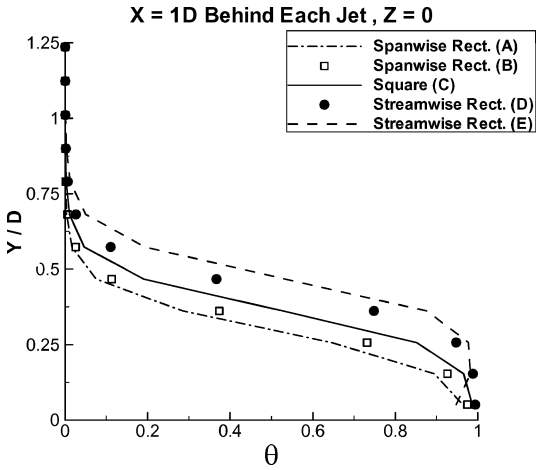

Fig. 13 Cooling efficiency at the position 1*D* behind the jet and at *Z* = 0, for the jet angle of 30 deg and velocity ratio of 0.5, using discrete holes injections with different aspect ratios.

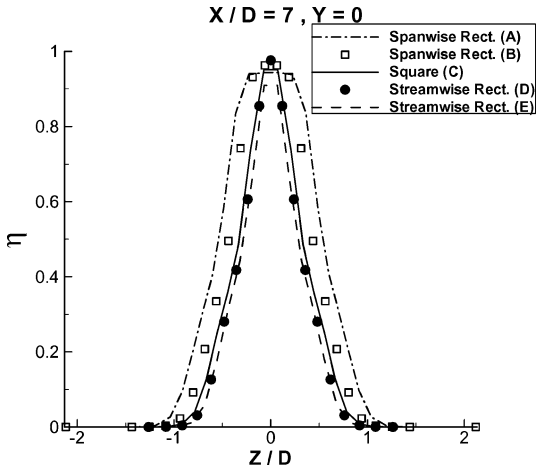

Fig. 14 Film-cooling effectiveness at *X* = 7*D* and *Y* = 0, for the jet angle of 30 deg and velocity ratio of 0.5, using discrete holes injections with different aspect ratios.

the jet spacing decreases the film-cooling effectiveness marginally in streamwise direction (especially up to about 6*D* downstream of the jet). Also, from Fig. 16, which indicates the spanwise spread of film cooling at $X = 6.5D$, it can be seen that increasing the jet spacing has a negligible effect on spanwise spread of film-cooling effects.

D. Comparison of Slot and Discrete Holes Injection Techniques

Figure 17, indicating a direct comparison between two types of film cooling, shows that the film-cooling efficiency of slot injection case is obviously higher with smaller slope. In other words, the slot injection has a steadier and longer film cooling even for the velocity ratio of 0.5 (which causes the weakest film cooling for slot injection and the strongest film cooling for the hole injection).

Another important difference between the two film-cooling approaches is the effect over the wall. At 90-deg jet injection angle, in the slot injection film cooling the height of the cooled fluid is about 1.8 times that of the second approach. Therefore, the disadvantage of influencing the cold fluid into the crossflow causes more damage in the slot injection film cooling than in the discrete holes approach, whereas for 30-deg jet injection angle the height of the jet in the slot injection method is less than that of the other method. In fact, at the jet injection angle of 30 deg, which is the optimal angle for both approaches, the slot injection creates a lower jet height and thus results in better film-cooling effectiveness at velocity ratios more than unity.

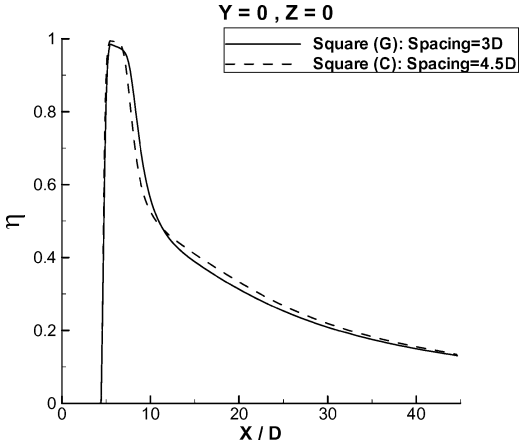

Fig. 15 Effects of jet spacing at the jet centerline (*Y* = 0, *Z* = 0) for the jet injection angle of 30 deg and velocity ratio of 0.5, using discrete holes injection.

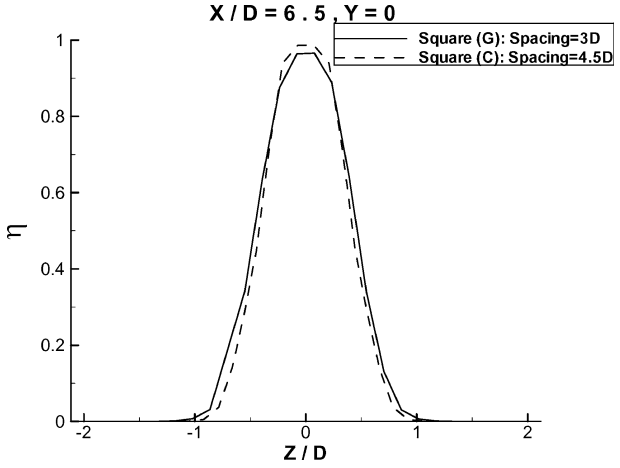

Fig. 16 Effects of jet spacing at *X* = 6.5*D* and *Y* = 0, for the jet injection angle of 30 deg and velocity ratio of 0.5, using discrete holes injection.

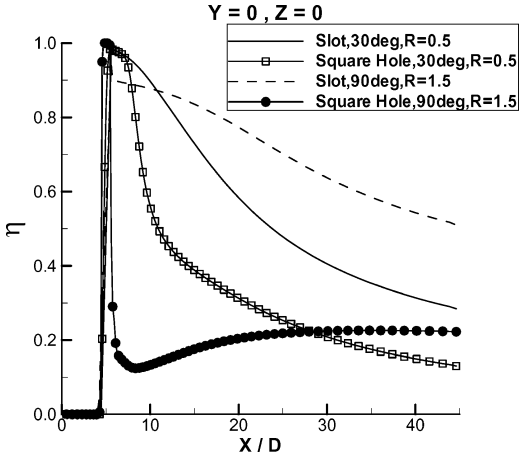

Fig. 17 Comparison of the results of two different types of film cooling, that is, slot and discrete holes injection (with spacing = 3*D*) at the centerline (*Y* = 0, *Z* = 0).

IX. Conclusions

In this work, two different methods of turbulent flat-plate film cooling, namely, slot injection and discrete holes injection, have been numerically studied. In each method, the effects of the velocity ratio and the jet injection angle have been studied. The results show a more efficient film cooling when slot injection is used. However, the slot injection causes structural problems, and thus there are practical limitations in its application. At the jet injection angle of 90 deg, the

physics of the flow behind the jet in discrete holes method is considerably different from that of the slot injection one. As a result, at 90-deg injection angle, in the slot injection method, the jet penetrates deeper into the main flow. However, at 30-deg injection angle the height of the jet in the slot injection case is less than that of the discrete holes injection one. However, in both methods the optimum film cooling occurs at the jet angle of 30 deg, with the velocity ratio of 1.5 for the slot injection and 0.5 for discrete holes one.

In discrete holes injection, the effects of the jet cross-section's aspect ratio was also investigated. The results show that changing the jet cross section from spanwise rectangle to streamwise rectangle decreases the effective film cooling along both streamwise and spanwise of the wall. Also, it increases the height of the cooled flow behind the jet. Thus, the flow far from the wall becomes cool resulting in higher aerodynamic losses. In addition, the more the rectangular section stretches in spanwise direction, the more rapidly the cooling effectiveness increases. Also, the study of the jet spacing shows that decreasing the jet spacing increases the cooling effectiveness, but not as much as changing the jet aspect ratio.

References

[1]Oates, G., *Aerothermodynamics of Aircraft Engine Components*, AIAA Education Series, AIAA, New York, 1985, Chap. 5.

[2]Cho, H., Kang, S., and Rhee, D. H., "Heat/Mass Transfer Measurement Within a Film Cooling Hole of Squared and Rectangular Cross Section," *Journal of Turbomachinery*, Vol. 123, No. 4, 2001, pp. 806–814.

[3]Gartshore, I., Salcudean, M., and Hassan, I., "Film Cooling Injection Hole Geometry: Hole Shape Comparison for Compound Cooling Orientation," *AIAA Journal*, Vol. 39, No. 8, 2001, pp. 1493–1499.

[4]Muldoon, F., and Acharya, S., "Numerical Investigation of the Dynamical Behavior of a Row of Squared Jets in Cross Flow over a Surface," American Society of Mechanical Engineering, Paper 99-GT-127, June 1999.

[5]Licu, D. N., Findlay, M., Gartshore, I., and Salcudean, M., "Transient Heat Transfer Measurements Using a Single Wide-Band Liquid Crystal Test," *Journal of Turbomachinery*, Vol. 122, No. 3, 2000, pp. 546–552.

[6]Goldstein, R. J., Eckert, E. R. G., Eriksen, V. L., and Ramsey, J. W., "Film Cooling with Injection Through Holes: Adiabatic Wall Temperatures Downstream of a Circular Hole," *Journal of Engineering for Power, Series A*, No. 4, Oct. 1968.

[7]Hassan, I., Findlay, M., Salcudean, M., and Gartshore, I., "Prediction of Film Cooling with Compound-Angle Injection Using Different Turbulence Models," CFD 98 Conference, CFD Society of Canada, Quebec City, Quebec, June 1998.

[8]Eckert, E. R. C., Goldstein, R. J., Patankar, S. V., and Simon, T. W., "Experimental and Computational Studies of Film Cooling with Compound Angle Injection," Heat Transfer Lab., Univ. of Minnesota, Technical Rept. SR021, May 1998.

[9]Bergeles, G., Gosman, A. D., and Launder, B. E., "The Near Field Character of a Jet Discharged Through a Wall at 90 to a Main Stream," *Journal of Heat Transfer*, Vol. 98, Aug. 1976, pp. 373–376.

[10]Pedersen, D., Eckert, E., and Goldstein, R., "Film Cooling with Large Density Difference Between the Mainstream and the Secondary Fluid Measured by the Heat-Mass Transfer Analogy," *Journal of Heat Transfer*, Vol. 99, No. 4, 1977, pp. 620–627.

[11]Afejuku, W. O., Hay, N., and Lampard, D., "Measured Coolant Distributions Downstream of Single and Double Rows of Holes," *Journal of Engineering for Gas Turbines and Power*, Vol. 105, No. 1, 1983, pp. 172–177.

[12]Holdman, J. D., and Walker, R. E., "Mixing of a Row of Jets with a Confined Crossflow," *AIAA Journal*, Vol. 15, No. 2, 1977, pp. 243–249.

[13]Kim, S., and Benson, T., "Fuid Flow of a Row of Jets in Crossflow—A Numerical Study," *AIAA Journal*, Vol. 31, No.5, 1993, pp. 806–811.

[14]Garg, V. K., and Gaugler, R. E., "Effect of Velocity and Temperature Distribution at the Hole Exit on Film Cooling of Turbine Blades," *Journal of Turbomachinery*, Vol. 119, No. 2, 1997, pp. 343–351.

[15]Katodani, K., and Goldstein, R. J., "On the Nature of Jets Entering a Turbulent Flow," *Journal of Engineering for Gas Turbines and Power*, Vol. 101, No. 3, 1979, pp. 459–465.

[16]Lutum, E., and Johnson, B., "Influence of the Hole Length to Diameter Ratio on Film Cooling with Cylindrical Holes," *Journal of Turbomachinery*, Vol. 121, No. 2, 1999, pp. 209–216.

[17]Hale, C. A., Plesniak, M. W., and Ramdhyani, S., "Film Cooling Effectiveness for Short Film Cooling Holes Fed by a Narrow Plenum," *Journal of Turbomachinery*, Vol. 122, No. 3, 2000, pp. 553–557.

[18]Ligrani, P. M., and Ramsey, A. E., "Film Cooling from Spanwise Oriented Holes in Two Staggered Rows," *Journal of Turbomachinery*, Vol. 119, No. 3, 1997, pp. 562–567.

[19]Goldstein, R. J., Cho, H. H., and Jabbari, M. Y., "Effect of Plenum Crossflow on Heat (Mass) Transfer near and Within the Entrance of Film Cooling Holes," *Journal of Turbomachinery*, Vol. 119, No. 4, 1997, pp. 761–769.

[20]Hoda, A., and Acharya, S., "Predictions of a Film Coolant Jet in Cross Flow with Different Turbulence Models," *Journal of Turbomachinery*, Vol. 122, No. 3, 2000, pp. 558–569.

[21]Keimasi, M. R., and Taeibi-Rahni, M., "Numerical Simulation of Jets in a Cross-Flow Using Different Turbulence Models," *AIAA Journal*, Vol. 39, No. 12, 2001, pp. 2268–2277.

[22]Amer, A. A., Jubran, B. A., and Hamdan, M. A., "Comparison of Different Two-Equation Turbulence Models for Prediction of Film Cooling from Two Rows of Holes," *Journal of Numerical Heat Transfer*, Pt. a, Vol. 21, No. 2, 1992, pp. 143–163.

[23]Ajersch, P., Zhou, J. M., Ketler, S., Salcudean, M., and Gartshore, I. S., "Multiple Jets in a Cross-Flow: Detailed Measurements and Numerical Simulations," American Society of Mechanical Engineering, Paper 95-GT-9, June 1995.

[24]Launder, B. E., and Spalding, D. B., *Lectures in Mathematical Models of Turbulence*, Lecture 5: Two-Equation Models of Turbulence, Academic Press, London, 1972, pp. 90–110.

[25]Launder, B. E., and Spalding, D. B., "The Numerical Computation of Turbulent Flows," *Journal of Computer Methods in Applied Mechanics and Engineering*, Vol. 3, No. 2, 1974, pp. 269–289.

[26]*Methodology: STAR-CD*, ver. 3.15, Computational Dynamics Limited, UK, 2001.

[27]Fric, T. F., and Roshko, A., "Vortical Structure in the Wake of a Transverse Jet," *Journal of Fluid Mechanics*, Vol. 279, 1994, pp. 1–47.